Wurtzite to Zinc Blende Phase Transition in GaAs Nanowires Induced by Epitaxial Burying

ARTICLE *in* NANO LETTERS · JULY 2008

Impact Factor: 13.59 · DOI: 10.1021/nl080319y · Source: PubMed

NANO LETTERS

2008
Vol. 8, No. 6
1638-1643

Wurtzite to Zinc Blende Phase Transition in GaAs Nanowires Induced by Epitaxial Burying

Gilles Patriarche, Frank Glas,* Maria Tchernycheva, Corinne Sartel, Ludovic Largeau, and Jean-Christophe Harmand*

Laboratoire de Photonique et de Nanostructures, CNRS, route de Nozay, 91460 Marcoussis, France

George E. Cirlin

St. Petersburg Physical Technical Centre of the Russian Academy of Sciences for Research and Education, Khlopina 8/3, 195220 St. Petersburg, Russia

Received February 1, 2008; Revised Manuscript Received April 1, 2008

ABSTRACT

We bury vertical free-standing core−shell GaAs/AlGaAs nanowires by a planar GaAs overgrowth. As the nanowires get buried, their crystalline structure progressively transforms: whereas the upper emerging part retains its initial wurtzite structure, the buried part adopts the zinc blende structure of the burying layer. The burying process also suppresses all the stacking faults that existed in the wurtzite nanowires. We consider two possible mechanisms for the structural transition upon burying, examine how they can be discriminated from each other, and explain why the transition is favorable.

Semiconductor nanowires (NWs) are promising building blocks for future photonic and electronic devices.[1] Much effort has recently been devoted to their fabrication using epitaxial growth techniques such as metal organic vapor phase epitaxy (MOVPE),[2,3] chemical beam epitaxy,[4] or molecular beam epitaxy (MBE),[5–7] in the presence of a catalyst. Indeed, metal particles deposited on the semiconductor surface can induce unidirectional crystal growth, a phenomenon well described since the 1960s.[8] Gold is the metallic element most commonly used to catalyze the growth of elemental, III−V, or II−VI NWs. Nowadays, wire diameters of a few nanometers are achieved[9] and carrier confinement effects have been reported.[7] However, the NWs resulting from such a catalyst-assisted growth very often have a peculiar crystalline structure: although the most stable crystal structure of many III−V and II−VI bulk materials is cubic sphalerite (or zinc blende, ZB), the same compounds often adopt the hexagonal wurtzite (WZ) structure when forming NWs. This phenomenon has been reported for most compounds and growth techniques[10,3,4,6,9,11] and several possible explanations have recently been discussed.[12–14] However, stacking faults (SFs),[3,4,11] twin planes,[10] and polytypes[6] are frequently observed, and it remains very challenging to synthesize NWs of a pure crystalline phase. Besides the problem of crystal phase control, some characteristics of free-standing NWs may turn into serious drawbacks for specific applications. For instance, their large surface to volume ratio makes their properties extremely sensitive to surface effects. This peculiarity is attractive for sensing applications, but on the other hand, optical and transport properties may suffer from instabilities or degradation related to surface states and surface oxidation (unwanted Fermi level pinning, nonradiative recombination centers). The electrical activity of doping impurities is another issue, since the ionization energy of dopants is expected to increase drastically with the reduction of the NW diameter.[15] In view of these problems, burying free-standing NWs in a condensed medium is an interesting solution to consider, which might prove important for technological issues, for instance the passivation of unwanted surface effects, as well as for fundamental studies, quantum electronic transport in particular. In order to retain the one-dimensional character of the NW, the burying material must differ from the NW material; alternatively, same-material burying is possible provided an intermediate shell has been grown around the NW. An MOVPE growth scheme was recently proposed to embed GaAs NWs into AlGaAs[16] or GaAs[17] and cross-sectional scanning tunneling microscopy was used to obtain

* Corresponding authors: Frank Glas, phone +33 1 69 63 60 79, fax +33 1 69 63 60 06, e-mail frank.glas@lpn.cnrs.fr; Jean-Christophe Harmand, phone +33 1 69 63 60 81, fax +33 1 69 63 60 06, e-mail jean-christophe.harmand@lpn.cnrs.fr.

10.1021/nl080319y CCC: $40.75
Published on Web 05/10/2008

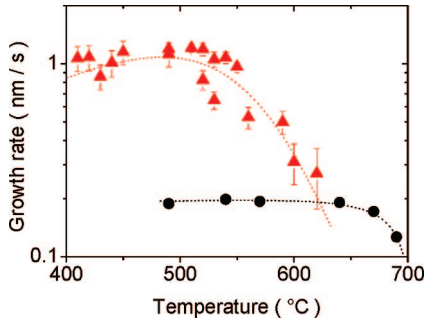

Figure 1. GaAs growth rates as a function of substrate temperature: comparison of Au-catalyzed NW growth (triangles) with 2D growth on a bare substrate (dots). The error bars give the dispersions measured over several samples.

detailed information on the resulting structures and to identify the dopants or impurities that they may contain.[17,18] In this work, we propose an MBE-based method to bury vertical AlGaAs/GaAs core−shell NWs into GaAs and we demonstrate a remarkable phenomenon, namely, that the GaAs burying overgrowth induces a phase transition of the NW crystalline structure from wurtzite to zinc blende. Because it suppresses all the stacking faults that existed in the wurtzite nanowires, this process is an efficient means to obtain NWs with a perfect single crystal structure.

Vertical NWs were grown by MBE on ($\bar{1}\bar{1}\bar{1}$) GaAs substrates. First, a thin Au film (0.5 nm) was deposited on a clean GaAs ($\bar{1}\bar{1}\bar{1}$) surface. Catalyst droplets were formed by annealing the sample at 500 °C. The formation of regular GaAs NWs occurs for substrate temperatures between 400 and 620 °C, a range within which the catalyst droplets are liquid and NW formation proceeds via vapor−liquid−solid (VLS) growth, as detailed elsewhere.[19] Concurrently to the VLS growth, a two-dimensional (2D) layer grows on the substrate surface between the NWs. The competition between these two growth modes is highly sensitive to the substrate temperature, as shown by Figure 1, which compares the temperature dependences of the growth rates of the NWs and of 2D layers formed under the same conditions, but on a bare (catalyst-free) GaAs substrate. On the bare substrate, the growth rate has a constant value of 0.2 nm/s up to 650 °C. Above this temperature, Ga desorption becomes significant and the growth rate starts to decrease.[20] Let us now consider the NWs. Between 400 and 520 °C, they grow 6 times faster than the reference 2D layer. Remarkably, their growth rate decreases steeply above 530 °C, a temperature well below the Ga desorption threshold observed on the bare substrate. At 630 °C, NW growth is inhibited whereas the growth of the reference 2D layer has not yet slowed down. The reason for these different kinetics will be discussed elsewhere. We thus end up with a range of temperature of 630−650 °C, where pre-existing NWs may be buried by a 2D overgrowth taking place on the remaining substrate surface.

The samples studied in this Letter were obtained as follows: (i) Vertical free-standing GaAs NWs were grown at 500 °C. (ii) The NWs were wrapped with $Al_xGa_{1-x}As$ shells ($x \sim 0.3$) at the same temperature. Because Al adatoms diffuse less than Ga, the deposition of AlGaAs is much less affected by the presence of the catalyst than that of GaAs. As a result, an AlGaAs layer forms on the substrate surface, on the NW sidewalls, and on top of the NWs by VLS growth. (iii) The resulting core−shell NWs were buried by a GaAs overgrowth performed at 640 °C. For comparison, samples were fabricated in the same conditions with partially or entirely buried NWs as well as with nonburied NWs. In partially buried NWs, the diameters of the buried and emerging parts are equal (30 nm on average), which shows that no significant lateral growth occurs on the NW sidewalls at the burying stage. Moreover, the average lengths of unburied and buried NWs are equal (1 μm), confirming that the VLS mechanism is inhibited during overgrowth. Therefore, the burying process only consists of epitaxial growth taking place on the substrate surface.

The structure of the NWs was determined by transmission electron microscopy (TEM). The samples were prepared as usual by first gluing face to face two bands cleaved along {1$\bar{1}$0} planes; the assembly was then polished mechanochemically and milled with Ar^+ ions at 5 keV (with final thinning at 2.5 keV). The specimens were examined in an FEI CM20 microscope operated at 200 kV. All the images were taken with the incident beam along a [1$\bar{1}$0] ZB ([11$\bar{2}$0] WZ) direction parallel to the substrate surface, which ensures that, when present, the SFs or twins are clearly visible.[2,4,21] Figure 2 shows TEM images of NWs before and after complete or partial burying. The free-standing NW of Figure 2a has the WZ structure, and several SFs are observed, as reported in other studies.[4,11] Figure 2b is a 002 dark field TEM image of an entirely buried NW. The faint contrast stems from the presence of Al in the shell.[22] The striking fact is that the burying layer and the NW have the same ZB crystalline structure. This can first be ascertained by examining the electron diffraction patterns (not shown), which are free of any additional spot specific to the WZ structure. It is further demonstrated in the corresponding high-resolution TEM (HRTEM) image, where only the plane stacking characteristic of ZB is visible (Figure 2c). Correlatively, the power spectrum of this image (bottom inset) shows only the spots characteristic of ZB. Moreover, the HRTEM specimen thickness is of the order of the NW diameter so that any structural difference between the NW and the burying material possibly stacked along the beam direction in the NW region (as schematized in the top inset for specimens thicker than the NWs) would manifest itself by moiré effects resulting from interferences between the beams diffracted by the two materials. Since the burying GaAs overgrowth took place on the ($\bar{1}\bar{1}\bar{1}$) cubic surface, its ZB structure has nothing surprising. On the other hand, the crystalline structure of the pre-existing NWs must have transformed from WZ (Figure 2a) to ZB (Figure 2b,c). Moreover, the NW is now free of any SF or twin plane, which would clearly appear in the TEM images.

Let us now observe a partially buried NW. Figure 2d clearly shows that the part of the NW emerging from the overgrowth retains the WZ structure whereas the buried part has switched to ZB. The interface between the two crystalline phases of the NW is very abrupt. This demonstrates that the

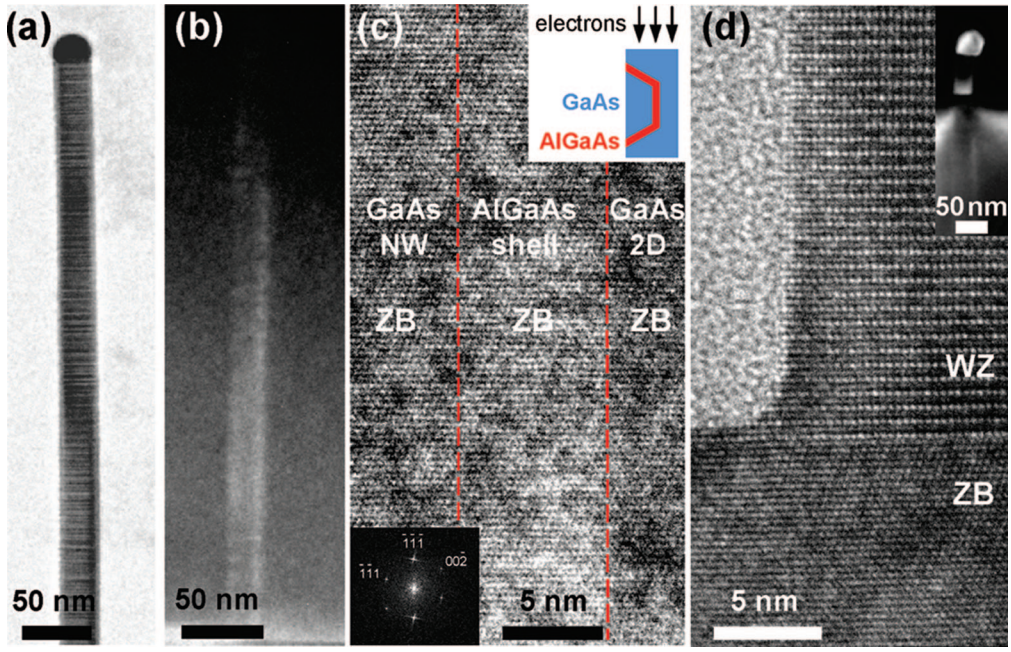

Figure 2. TEM images of GaAs nanowires with [$\bar{1}\bar{1}\bar{1}$] growth axis upward: (a) bright field image of a nonburied nanowire; (b) 002 dark field image of a completely buried nanowire; (c) HRTEM image of the interface region between GaAs core, AlGaAs shell, and burying GaAs (Each dot is the image of a pair of III−V columns seen edge-on. The location of the AlGaAs shell, visible only as a slightly brighter ill-defined layer (as expected from the low contrast between GaAs and AlGaAs and from the specimen geometry, see top inset) was cross-checked by medium-resolution TEM imaging. The bottom inset is a computed power spectrum of the image of the NW region.); (d) HRTEM image of the interface region between the buried (bottom) and unburied (top) portions of the nanowire. The inset shows a partially buried NW at lower magnification.

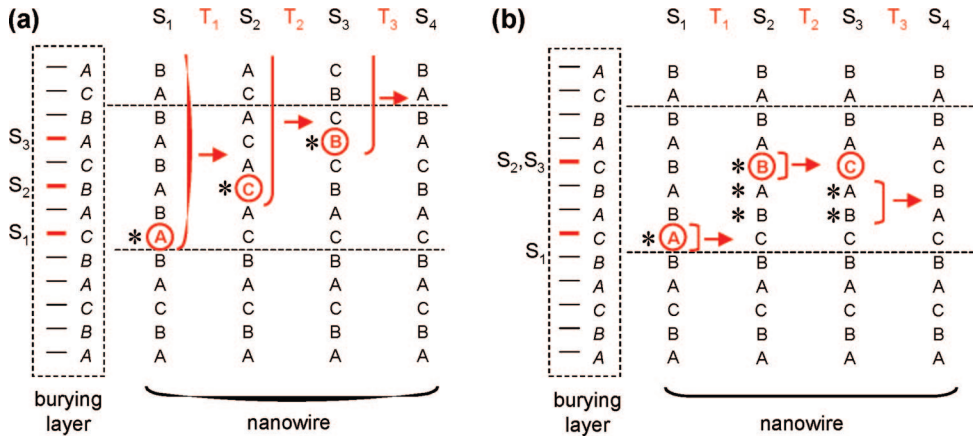

Figure 3. Transformations of a wurtzite nanowire into zinc blende: (a) type I, (b) type II. The stacking in the zinc blende burying layer is given in the dashed boxes at left. The next four columns show the stacking in the nanowire at various stages S_i of each process, composed of elementary transformations T_i. Final stage S_4 is equivalent to initial stage S_1. The level reached by the burying layer at each stage is marked by a thick line (burying layer) and a circle (nanowire). Brackets and arrows indicate which MLs are translated at each stage. Stars denote the height location of the linear defects.

structural phase transition is not an effect of thermal annealing of the wires during the overgrowth at 640 °C, which would also have transformed the crystalline structure of the emerging part. Our observations indicate that, on the contrary, the phase transition occurs step by step, when the overgrowth atomic layers meet the NW sidewalls. We shall address two questions. First, how is this transformation realized at the atomic scale? Second, why does it happen?

To this end, we consider the burying process in more detail. Recall that ZB and WZ structures may be described as stacks along the [$\bar{1}\bar{1}\bar{1}$] growth direction of identical monolayers (MLs), each made of two planes of atoms belonging respectively to columns III (below) and V (above). The structures differ by the lateral positioning of the MLs. The two stacking modes are usually noted ABCABC... (ZB) and ABABAB... (WZ), where the letters represent distinct lateral positions of a ML[23] (Figure 3). In both structures, any column-III atom sits directly above the column-V atom of the underlying ML; the A, B, or C character of each ML is therefore entirely determined by the lateral positioning of its column-V atoms. Let us assume that the burying process has already transformed the lower part of the NW to the ZB

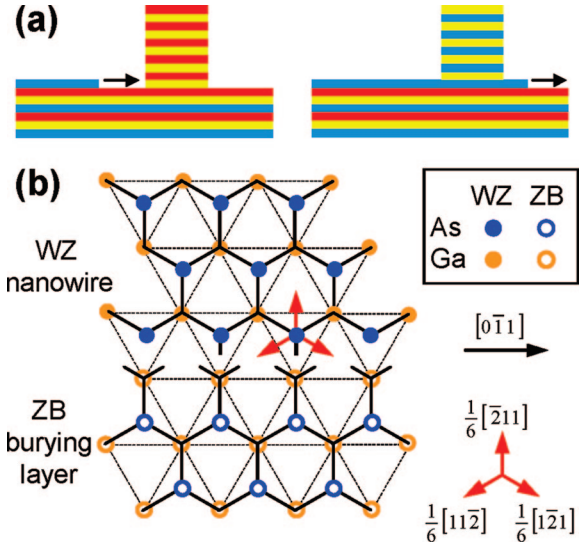

Figure 4. Top monolayer of the zinc blende burying layer meeting the corresponding monolayer of the nanowire in an out-of-registry condition. (a) Side view before (left) and after (right) a type I phase transformation. Each color denotes a different ML lateral position. (b) Top view. The partial dislocation created at the boundary can be annihilated by any of three translations of the nanowire monolayer (red arrows), indexed in the zinc blende lattice.

stacking, in lateral registry with the stacking of the burying layer (Figure 3, stage S_1). Since the smallest period common to WZ and ZB is 6 MLs long, we shall consider how the next sequence of six unburied WZ MLs ABABAB (between the dashed lines) may transform into ZB sequence CABCAB upon burying.

When the top ML of the burying GaAs reaches the side of the NW by step flow growth (Figure 4a, left), the lateral positioning of the As atoms in the burying ML and in the corresponding ML of the NW (the first in the sequence of 6 MLs) are not in registry, as opposed to the underlying Ga atoms whose positions are fixed by the ZB structure common to the overgrowth and to the already transformed NW (Figure 4b). The simplest way to correct this fault is to shift rigidly the whole emerging part of the NW situated above (and including) this As plane (Figure 3a, transformation T_1). This puts two more MLs in the correct ZB position (Figures 3a and 4a). When the burying layer reaches the level of the next faulted plane, two MLs above the previous one, the same process repeats (Figure 3a, transformation T_2 at stage S_2), and so on every other ML. At each step, three equivalent translation vectors are permitted, namely, $^1/_6[\bar{2}11]$, $^1/_6[11\bar{2}]$, and $^1/_6[1\bar{2}1]$ (Figure 4b).

This type I process can also be described in terms of dislocations. Our NWs indeed have hexagonal sections and vertical sidewalls parallel to the $\{10\bar{1}0\}$ WZ planes ($\{\bar{2}11\}$ ZB planes), as commonly observed for GaAs WZ NWs of small diameter.[24,25] The edges of the NW MLs are thus along the $\langle 1\bar{1}0\rangle$ directions. The lateral contact between the top burying ML and the corresponding NW ML (at stages S_1, S_2, or S_3) produces a linear crystalline defect at the boundary between the two crystalline phases. With respect to the ZB structure, this defect may be considered as a Shockley partial dislocation, composed of segments lying along $\langle 1\bar{1}0\rangle$ directions[23,26] (even though it is only partially surrounded by material) and bordering the faulted As plane. As the dislocation glides along the $(\bar{1}\bar{1}\bar{1})$ plane into the NW, the first NW As atoms close to the lateral boundary shift into ZB position. The translation of the whole As layer fully eliminates dislocation and stacking fault. The Burgers vector of the partial dislocation is one of the three translations identified above (or their opposites, depending on orientation conventions).

The transformation of WZ into ZB via repeated type I plane translations was considered long ago in the context of mineralogy of bulk samples (although no description in terms of dislocations was given), in which case ZB nuclei must form in the WZ matrix.[27] The NW geometry and the progressive burying make the situation very different here. Moreover, the type I process was deemed as the only one that can operate for the sustained transformation of WZ into ZB, other mechanisms leading to the formation of metastable polytypes.[27] However, we note that a more intricate type II process may occur whereby only one or two MLs of the NW are translated at each step, the lateral positions of all the other MLs remaining unaffected (Figure 3b). The same partial dislocation is generated at stage S_1 but transformation T_1 is now the translation of the sole NW ML that it borders. This eliminates the fault in this ML but also modifies the fault situated two MLs above, since the local stacking in the NW becomes ABCBA (stage S_2), characteristic of a twin plane or of an extrinsic SF in the ZB structure. The next two NW MLs cannot be transformed before the third one, when the burying material reaches its level (stage S_2; the linear defect between ZB overgrowth and NW is then 3 MLs high), again by translation of a single ML (T_2), producing a "double-twin" sequence ABCBACAB in the NW. Finally, the two already buried intermediate MLs can transform (T_3).

These two types of processes transforming WZ into ZB can be distinguished by HRTEM via differences in stacking sequences at the interface between the untransformed and transformed parts of the NW. We first identify the last MLs that adopt the stacking sequence of the ZB overgrowth in the transformed part of the NW. At any stage of a type I process (Figure 3a), the next two MLs repeat the last two MLs of the ZB sequence (e.g., ABCA followed by CA at stage S_2) whereas during a type II process, the same sequence (characteristic of an intrinsic SF in ZB[23]) is found only at stage S_1, other well-defined twinlike sequences occurring at stages S_2 and S_3 (Figure 3b). In the many HRTEM images examined, we found only the stacking sequence characteristic of the type I process (Figure 5) and no evidence of the other sequences that should occur in a type II process (Figure 3b). This indicates that, at least for GaAs and in our burying conditions, type I is the dominant transformation mechanism, if not the only one.

If the three translations allowed for each ML are equiprobable, and because their sum is zero (Figure 4b), the tilt angle θ with respect to the substrate, averaged over an ensemble of NWs each constituted of N MLs, is zero and the variance of its tangent is $\langle \tan^2\theta\rangle = 1/(8N)$. For 1 μm long NWs, the corresponding angle is only 0.37°. This is compatible

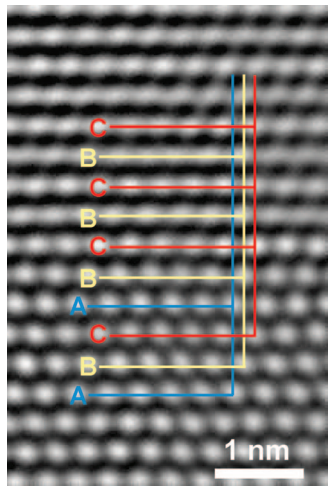

Figure 5. Fourier-filtered HRTEM image showing the detail of the stacking sequence at the buried/unburied interface of a GaAs NW, with identification of the lateral positions of the monolayers.

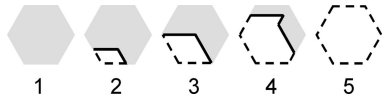

Figure 6. Arbitrary stages of the transformation of a nanowire ML from wurtzite stacking position into zinc blende position (top view). The faulted (untransformed) area is shaded. Solid lines indicate the progression of the linear defect initially formed (dashed line) at the boundary between burying ML and nanowire sidewall. The length ratio of solid to dashed lines equals 1 up to stage 3 and then decreases. Regarding the SF, its area constantly decreases.

with the fact that we do not detect any significant tilt in our buried NWs (Figure 2b). Which translation is selected for each ML probably depends on which NW facet is first reached by the advancing burying ML and on the precise atomic structures of the latter and of the NW sidewall.

We now demonstrate that the transformation of the NW WZ structure into ZB not only is thermodynamically favorable but also becomes kinetically allowed in the presence of the burying layer. We consider only the type I process, but similar arguments apply to the type II process. Two interdependent features contribute to the change of energy of the system during the transformation, namely, the partial dislocation segments initially formed between burying layer and NW and the faulted interface between the transformed and untransformed parts of the NW. Figure 6 describes schematically how dislocation and fault are modified during the transformation of each ML. As overgrowth proceeds, the NW sidewalls are progressively surrounded by the top burying ML extending by step flow. The partial dislocation is thereby generated at the periphery of the corresponding NW ML. As soon as the dislocation has formed along at least two sides of the hexagon, it is possible for any of its parts to move inward without any length increase and therefore, as a first approximation, without any energy increase. The area of the NW ML swept by the dislocation transforms to ZB stacking with respect to the underlying ZB portion of the NW. Using Geilikman's model for the energetics of the phases intermediate between WZ and ZB, which takes into account interactions between neighboring MLs,[27] together with a computed value of the difference of cohesive energies between bulk ZB and WZ GaAs,[28] we find that eliminating the fault corresponds to a decrease of energy of about 28 $mJ \cdot m^{-2}$ (since the complete transformation of the NW into ZB requires eliminating the same fault every second ML, this is exactly the difference of cohesive energies per 2 ML slab of NW). Hence, the total energy associated with the defects continually decreases during each elementary transformation T_i of a ML (Figure 3). According to this analysis, there would be no energy barrier to the transformation. We believe that this might explain why the transformation occurs very rapidly when the top burying ML comes in contact with a NW, leading to abrupt interfaces between the transformed and untransformed parts of the NW (Figures 2d and 5). Moreover, there is no critical NW radius for the transformation, which explains why the structure of any NW shifts to ZB. However, this simple picture neglects the Peierls energy barriers impeding the glide of the partial dislocation[26] and the possible variation of its energy per unit length due to changes in its environment as it starts to penetrate into the NW. Both effects might introduce kinetic barriers to the transformation. Of course, when a NW ML is already in the correct ZB position, no dislocation is created and hence no driving force for translating the layer. This happens in particular when there is a fault (SF or twin boundary) or a ZB segment in the NW before burying and explains why all such pre-existing defects (Figure 2a) get eliminated (Figure 2b).

Further work is needed to assess the applicability of the current method to other materials. On the one hand, we believe that the VLS growth should be systematically inhibited at lower temperature as compared to the 2D growth (this will be discussed elsewhere). A growth temperature window compatible with NW burying should thus exist for any material system. On the other hand, the capability of free-standing NWs to accommodate a large misfit between the various materials involved[29] is partially lost when applying the present burying process. Other advantages of the free-standing geometry such as ease of handling and probing capability could be recovered, albeit now with a NW free of any of the extended defects that often plague as-grown NWs. To achieve this, it would suffice to eliminate the burying material by etching, using the shell as an etch-stop layer. Finally, as already mentioned, specific advantages of buried NWs could manifest themselves in the physics of electronic transport in a defect-free one-dimensional semiconductor channel.

In conclusion, we have observed and explained how NWs standing vertically on their substrate and having the wurtzite crystalline structure can be buried by epitaxial overgrowth and transformed to the zinc blende structure. We examined the case of GaAs/AlGaAs core/shell NWs initially grown by VLS and then buried by GaAs. The burying process is efficient in a narrow temperature range (630−650 °C) where VLS growth is inhibited while 2D growth persists at the substrate surface. The crystalline phase transition of the NWs was found to occur step by step. Each new ML growing by step flow at the ZB substrate surface induces a translation

of the emerging part of the NW that it meets, if the corresponding NW ML is out of registry. This translation brings the NW ML in registry with the ZB position of the growing ML. This mechanism is repeated as long as overgrowth proceeds. When the burying layer is fault-free, this suppresses all the SFs pre-existing in the NW. Complete burying results in perfect ZB GaAs NWs with their AlGaAs shells embedded in the overgrown GaAs matrix.

Acknowledgment. This work was partly supported by the SANDIE Network of Excellence of the European Commission (Contract # NMP4-CT-2004-500101) and by Agence Nationale de la Recherche (Contract Filemon35).

References

(1) Li, Y.; Qian, F.; Xiang, J.; Lieber, C. M. *Mater. Today* **2006**, *9*, 18–27.
(2) Hiruma, K.; Yasawa, M.; Haraguchi, K.; Ogawa, K.; Katsuyama, T.; Koguchi, M.; Kakibayashi, H. *J. Appl. Phys.* **1993**, *74*, 3162–3171.
(3) Mohan, P.; Motohisa, J.; Fukui, T. *Nanotechnology* **2005**, *16*, 2903–2907.
(4) Persson, A. I.; Larsson, M. W.; Stenstrom, S.; Ohlsson, B. J.; Samuelson, L.; Wallenberg, L. R. *Nat. Mater.* **2004**, *3*, 677–681.
(5) Wu, Z. H.; Mei, X. Y.; Kim, D.; Blumin, M.; Ruda, H. E. *Appl. Phys. Lett.* **2002**, *81*, 5177–5179.
(6) Soshnikov, I. P.; Cirlin, G. E.; Tonkikh, A. A.; Samsonenko, Y. B.; Dubrovskii, V. G.; Ustinov, V. M.; Gorbenko, O. M.; Litvinov, D.; Gerthsen, D. *Phys. Solid State* **2005**, *47*, 2121–2126.
(7) Chen, C.; Shehata, S.; Fradin, C.; LaPierre, R.; Couteau, C.; Weihs, G. *Nano Lett.* **2007**, *7*, 2584–2589.
(8) Wagner, R. S.; Ellis, W. C. *Appl. Phys. Lett.* **1964**, *4*, 89–90.
(9) Duan, X.; Lieber, C. M. *Adv. Mater.* **2000**, *12*, 298–302.
(10) Koguchi, M.; Kakibayashi, H.; Yasawa, M.; Hiruma, K.; Katsuyama, T. *Jpn. J. Appl. Phys.* **1992**, *31*, 2061–2065.
(11) Harmand, J. C.; Patriarche, G.; Péré-Laperne, N.; Mérat-Combes, M.-N.; Travers, L.; Glas, F. *Appl. Phys. Lett.* **2005**, *87*, 203101.
(12) Akiyama, T.; Sano, K.; Nakamura, K.; Ito, T. *Jpn. J. Appl. Phys.* **2006**, *45*, L275–L278.
(13) Glas, F.; Harmand, J.-C.; Patriarche, G. *Phys. Rev. Lett.* **2007**, *99*, 146101.
(14) Dubrovskii, V. G.; Sibirev, N. V. *Phys. Rev. B* **2008**, *77*, 035414.
(15) Diarra, M.; Niquet, Y.-M.; Delerue, C.; Allan, G. *Phys. Rev. B* **2007**, *75*, 045301.
(16) Mikkelsen, A.; Sköld, N.; Ouattara, L.; Borgstrom, M.; Andersen, J. N.; Samuelson, L.; Seifert, W.; Lundgren, E. *Nat. Mater.* **2004**, *3*, 519–523.
(17) Ouattara, L.; Mikkelsen, A.; Sköld, N.; Ericsson, J.; Knaapen, T.; Cavar, E.; Seifert, W.; Samuelson, L.; Lundgren, E. *Nano Lett.* **2007**, *7*, 2859–2864.
(18) Mikkelsen, A.; Sköld, N.; Ouattara, L.; Lundgren, E. *Nanotechnology* **2006**, *17*, S362–S368.
(19) Tchernycheva, M.; Harmand, J.-C.; Patriarche, G.; Travers, L.; Cirlin, G. E. *Nanotechnology* **2006**, *17*, 4025–4030.
(20) Van Hove, J. M.; Cohen, P. I. *Appl. Phys. Lett.* **1985**, *47*, 726–728.
(21) Johansson, J.; Karlsson, L. S.; Svensson, C. P. T.; Martensson, T.; Wacaser, B. A.; Deppert, K.; Samuelson, L.; Seifert, W. *Nat. Mater.* **2006**, *5*, 574–580.
(22) Petroff, P. M. *J. Vac. Sci. Technol.* **1974**, *14*, 973–978.
(23) Bollmann, W. *Crystal defects and crystalline interfaces*; Springer: Berlin, 1970.
(24) Plante, M. C.; LaPierre, R. R. *J. Cryst. Growth* **2006**, *286*, 394–399.
(25) Mariager, S. O.; Sørensen, C. B.; Aagesen, M.; Nygård, J.; Feidenhans'l, R.; Willmott, P. R. *Appl. Phys. Lett.* **2007**, *91*, 083106.
(26) Hirth, J. P.; Lothe, J. *Theory of dislocations*, 2nd ed.; Wiley: New York, 1982.
(27) Geilikman, M. B. *Phys. Chem. Miner.* **1982**, *8*, 2–7.
(28) Yeh, C.-Y.; Lu, Z. W.; Froyen, S.; Zunger, A. *Phys. Rev. B* **1992**, *46*, 10086–10097.
(29) Glas, F. *Phys. Rev. B* **2006**, *74*, 121302.

NL080319Y